Performing self propelled simulations of a kayak, using a Body-force paddle model

J. Banks*, A.B. Phillips, S.R. Turnock, D.A. Hudson
*jb105@soton.ac.uk

1 Introduction

Understanding the interactions between a hull and a propeller is a common problem naval architects have to solve to provide efficient powering solutions. The world of elite sport is becoming increasingly scientific in a similar drive for increased performance. To allow a kayak's hull and paddle to be optimised, their interactions have to be considered to provide a realistic race scenario. It is therefore proposed that numerical techniques currently used by naval architects could be applied to the problem of a self propelled kayak.

The computational cost of fully resolving the flow around a rotating propeller and hull inhibits the use of numerical simulations for commercial use. However, several groups have implemented simplified body force propeller models, which accurately induce the accelerations produced by a propeller into the fluid (Phillips et al, 2010). A similar body force methodology is adopted to simulate the impact a paddle stroke has on the fluid around a moving kayak. This is done using the open source CFD package OpenFOAM (OpenFOAM, 2009).

2 Theoretical approach

A finite volume method is adopted, using a Volume of Fluid (VOF) approach for the free surface. This method is derived from the surface integration of the conservative form of Navier Stokes' equations over a control volume. The incompressible Reynolds averaged Navier-Stokes (RANS) equations, written in tensor form, are defined as

$$\frac{\partial(\rho U_i)}{\partial t}+\frac{\partial(\rho U_i U_j)}{\partial x_j}=-\frac{\partial P}{\partial x_i}+\frac{\partial}{\partial x_j}\left[\mu\left(\frac{\partial U_i}{\partial x_j}+\frac{\partial U_j}{\partial x_j}\right)\right] -\frac{\partial}{\partial x_j}\left(\rho\overline{u'_i u'_j}\right)+f_i \qquad \text{2-1}$$

and

$$\frac{\partial U_i}{\partial x_i}=0 \qquad \text{2-2,}$$

for momentum and mass continuity respectively. While the volume fraction transport equation is defined as

$$\frac{\partial c}{\partial t}+\frac{\partial(cU_j)}{\partial x_j}=0 \qquad \text{2-3,}$$

where c is the volume fraction defined as (V_{air}/V_{total}) (Peric and Ferziger, 2002).

The fluid density, ρ, and viscosity, μ, can then be calculated as

$$\rho=\rho_{air}c+\rho_{water}(1-c) \qquad \text{2-4}$$

and

$$\mu=\mu_{air}c+\mu_{water}(1-c) \qquad \text{2-5}$$

respectively.

External forces applied to the fluid are represented as f_i, which include buoyancy forces and momentum sources representing the influence of the paddle. The effect of turbulence is represented in equation 2-1 by the Reynolds stress tensor $\rho\overline{u'_i u'_j}$ and is modelled using the k-omaga SST turbulence model contained within OpenFOAM-1.6 (OpenFOAM, 2009).

The SST model blends a variant of the k-ω model in the inner boundary layer and a transformed version of the k-ε model in the outer boundary layer and the free stream (Menter, 1994). This has been shown to be better at replicating the flow around the stern of a ship, than simpler models such as k-ε, single and zero equation models (Larsson et al, 2000)(Hino, 2005).

3 Body force Paddle model

3.1 Simple mathematical force model

To start with the fluid forces generated by the paddle blade were calculated based on a simple mathematical model of a flat plate rotating around a point moving with an advance speed of U_0 (see Figure 3-1). The angle of rotation θ is measured from the horizontal, in the direction of movement (i.e. increases throughout the stroke).

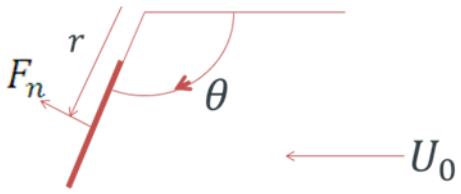

Figure 3-1 - free body diagram of paddle model.

The normal velocity encountered by the blade at a radius r is given by

$$V_n = (\dot{\theta} \times r - U_0) \cdot \hat{n} \qquad \textbf{3-1,}$$

where $\hat{n}$ is the unit vector normal to the blade calculated as

$$\hat{n} = \hat{\theta} \times \hat{r} \qquad \textbf{3-2.}$$

It follows, therefore that the hydrodynamic force on a length of blade *dr* ,at a radius *r* is given by

$$F_n = {}^1/_2 \rho (V_n)^2 C_D c.dr \cdot \hat{n} \qquad \textbf{3-3,}$$

where ρ is the density of water, C_D is the drag coefficient and *c* is the chord of the blade at *r*.

3.2 Calculating momentum source strengths from paddle force model

To represent the impact of the paddle on the fluid, the calculated paddle forces are applied to a propulsive domain located within the fluid. This domain represents the swept area of the paddle defined by the length (R) and the width (c). An inner radius can also be defined to account for the length of the paddle handle. The propulsive domain is then divided up into sectors of radius dR and angle dθ, this is demonstrated in Figure 3-2.

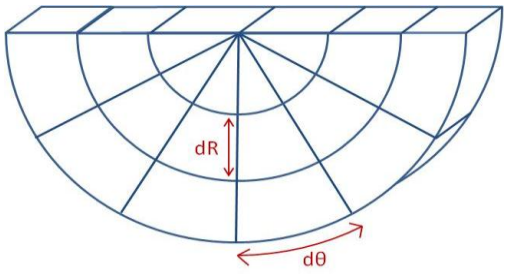

Figure 3-2 - Schematic of stroke propulsive domain divided into sectors.

When the paddle blade passes through a sector, the paddle force (F_n) is calculated for a section of blade, with length and chord equal to the sector dimensions, located at the centre of that sector. The momentum source term for that sector is then calculate as

$$\frac{F_n}{SectorVolume}.$$

Obviously as dr and dθ get smaller the propulsion model better represents a paddle moving smoothly through the water.

3.3 Applying source terms within OpenFOAM

The standard multiphase solver interFoam was modified to accommodate momentum source terms and renamed mom_interFoam. A new module within the solver was created 'createBodyForce.H' which is called every time step from within the top level solver program 'mom_interFoam.C'.

The parameters that define the propulsive model are defined within a dictionary located within the case files.

The propulsion domain is defined by the paddle dimensions, centre of rotation and unit vectors providing the direction of forward motion and the roll angle. The polar coordinates of the centre of each cell within the mesh are then calculated relative to the paddle centre of rotation. These are then used to determine which cells are within a given sector of the propulsive domain providing an accurate sector volume.

The run time of the current time step is then used to calculate the position of the paddle within the

propulsive domain, based on prescribed paddle angles throughout a single stroke cycle and a defined stroke rate. This is used to calculate the angular velocity of the paddle using the paddle position form the previous time step.

For each cell, within a sector containing the paddle, the momentum source term is calculated using the paddle force calculated for that sector divided by the sector volume. The source term for all other cells are set to zero. These source terms are stored within a volume vector field which is then added to the momentum equation (Ueqn.H within openFoam). The total paddle force is determined for each time step by multiplying each cell's source term with its cell volume and summating over the propulsive domain. The instantaneous thrust is then acquired by resolving this force into the direction of movement.

3.4 Experimental data

Experimental data for a rotating paddle was obtained as part of a student research project at the University of Southampton (Ellison, 2010). A kayak paddle was mounted on an instrumented pivot mechanism attached to a towing tank dynamometer (Figure 3-3). This allowed lift, drag and rotation angle to be recorded against time. A constant torque was applied to the paddle via a dropping weight allowing the dynamic forces generated by the blade to be measured against time. Various angles of attack were tested with a range of torques.

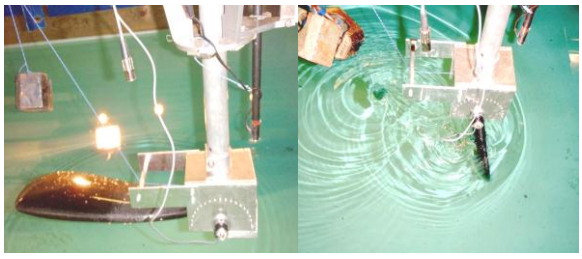

Figure 3-3 - Experimental setup for paddle test.

The experimental data for the blade at 90 degrees to the flow can be seen in Figure 3-4. Due to the blade starting out of the water, it accelerates quickly at first, entering the water at a high velocity resulting in a peak in the thrust at this point. A small blip in the angle data, at approximately 110 degrees from the horizontal, is thought to be due to the rotary potentiometer and not the flow physics. This error gets amplified when the angular velocity is calculated.

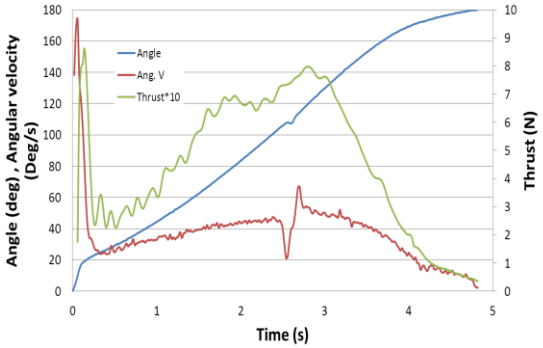

Figure 3-4 - Experimental data for a rotating paddle.

3.5 Validation against experimental data

The paddle that was used in the experiments was represented as a flat plated of the same length and chord (0.54 and 0.2m respectively). A flat plate drag coefficient of 1.2 was used as an initial approximation (Hoerner, 1965) whilst the propulsion domain was divided into 18 angular and 8 radial divisions, with an inner radius of 0.1m.

To start with the centre of rotation was placed on the surface of the water, so as to remove the complications of paddle entry. The angular velocity was maintained at a constant value throughout the stroke, determined as the average angular velocity from the experimental paddle stroke.

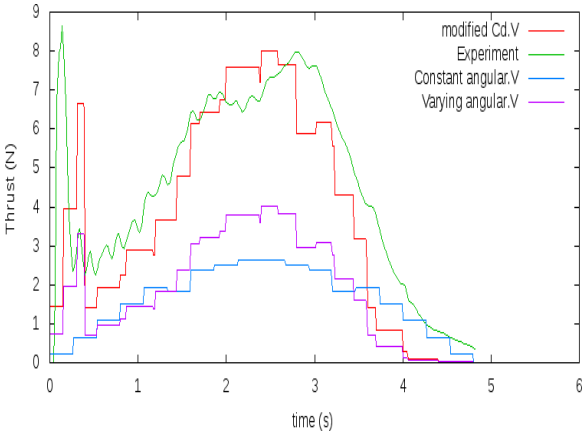

Figure 3-5 - Thrust generated by propulsive model compared with experimental data.

Out of a crude mesh of 40,000 cells, 740 were contained within the propulsive domain.

It can be seen in Figure 3-5 that the constant velocity propulsion model significantly underestimates the thrust measured in the experiment. However it is not just the magnitudes which do not match, the general shape of the curves differ significantly. To try and improve the paddle model the blade angle data that was recorded during the experiment was used to prescribe the paddle motion during the stroke. This modified thrust data can also be seen in Figure 3-5. Despite the magnitude of the thrust being approximately half that of the experimental data it can now be seen that the general trends aligns much more closely. This is easier to in the final thrust trace, where the drag coefficient has been doubled to 2.4.

There are many improvements that need to be made to the body-force model that could account for the discrepancies between the experimental data. Predominantly these would focus on including added mass terms to the mathematical model, so as to include unsteady flow features, and to remove the step-like variation in thrust through a smoother implementation of source terms within the fluid domain.

3.6 Applying two propulsion models within the same simulation

A second paddle model was easily added to the modified solver by having two identical modules that independently calculate momentum sources. The only difference is that the second paddle has a different centre of rotation and applies a phase shift to the prescribed paddle motion so that they are out of phase (typically 180 degrees).

4 Self propelled Simulation

4.1 Numerical model

The solver settings and simulation parameters can be found in Table 4-1.

Table 4-1 - Numerical settings

Property	Mesh
Type of mesh	Unstructured (Hexahedral)
No. of elements	Approximately 1.2M
y+ on the hull	10-15
Domain Physics	Homogeneous Water/Air multiphase, kOmegaSST turbulence model, Automatic wall function
Boundary physics:	
Inlet	Free stream velocity of 2m/s
Outlet	Zero gradient
Bottom/side wall	Wall with free stream velocity
Top	Opening
Hull	Wall with no slip condition
Solver settings:	
Transient scheme	1st order Euler
Grad (U) Scheme	Gauss linear
Div (U)	Gauss limitedLinearV 1
Pressure coupling	PISO
Convergence criteria	P 1e-7, U 1e-6, k 1e-8, omega 1e-8
Multiphase control	Volume fraction coupling
Timestep control	max Courant No = 0.4
Processing Parameters:	
Computing System	Iridis 3 Linux Cluster (University of Southampton)
Run type	Parallel (9 - 24 Partitions run on 5x8 core nodes each with 23 Gb RAM)

4.2 Meshing Technique

An unstructured hexahedral mesh around the kayak was created using the snappyHexMesh utility within OpenFOAM. Firstly a coarse block mesh of hexahedral cells is created, using the blockMesh utility, defining the size of the domain and the initial cell size in each direction. Specific areas within the domain are then specified for mesh refinement in progressive layers. For each layer of refinement conducted each cell within the specified region is split into 8 equal parts, doubling the mesh density in all directions. However uni-directional refinement was used across the free surface to provide good wave pattern resolution, whilst minimising computational cost. Boundary layer element are also grown out from the kayak surface mesh.

This localised refinement process results in a general mesh structure that can be seen in **Error! Reference source not found.**. It should be noted that the images of the mesh are generated using Paraview which currently displays hexahedral cells as two tetrahedral cells. The mesh is actually fully hexahedral.

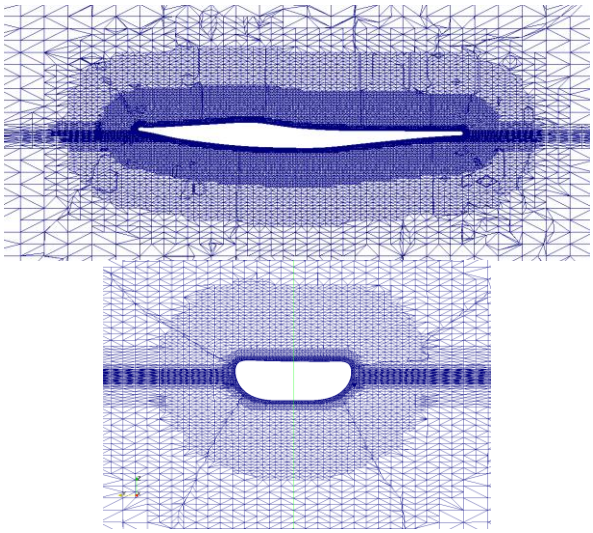

Figure 4-1 - Kayak mesh structure.

4.3 Naked hull resistance

The naked hull resistance of the kayak was determined to be 22.68 N. The resulting free surface deformation can be seen in Figure 4-2.

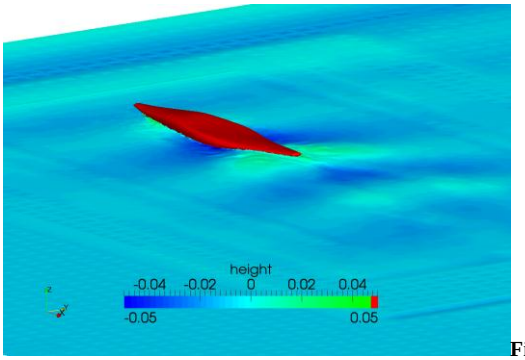

Figure 4-2 - Free surface deformation for naked hull kayak simulation

4.4 Determining the self propelled stoke rate

The naked hull resistance case files could then be used as an initial condition for the self propelled simulation. For this first attempt a self propelled kayak a fixed stroke rate was selected that would provide a thrust approximately equal to the naked hull resistance. In time this will become an iterative process varying stroke rate to match the self propelled resistance.

Without access to real stroke path data, the rate of angular velocity throughout the stroke was modelled as being sinusoidal, with zero angular velocity on paddle entry and exit. This provides a crude approximation of how an athlete might vary the velocity of the paddle to take account of the kayak's forward speed. The resulting force trace for a single paddle operating at a stroke rate of 40 can be seen in Figure 4-3. This happened to provided an average thrust of 11.3 N, so with two paddles operating out of phase with each other the average thrust would be 22.6 N. This was assumed to be close enough to the naked hull resistance of for the purposes of this study.

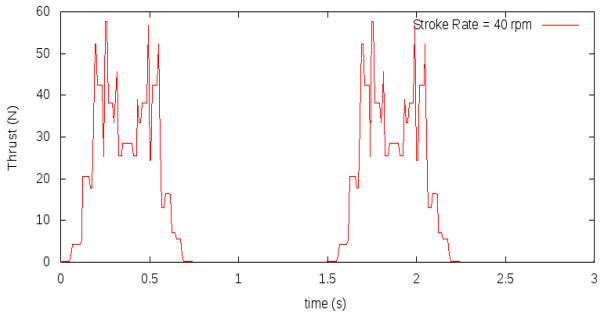

Figure 4-3 - thrust generated by a single paddle, with a sinusoidal angular velocity, against time

4.5 Paddle-hull interactions

The paddle induced velocities alongside the kayak can be seen in Figure 4-4, while their effect on the pressure field over the hull can be seen in Figure 4-5. Although this simulation far from replicates a realistic paddle stroke the interaction between the paddle and the hull an be clearly seen.

To see the impact this change in pressure field has on the kayak you have to look at the hydrodynamic forces and moments acting on the hull. In Figure 4-6 you can see how the side force varies throughout the stroke. As the paddle passes the right hand side of the hull, the pressure drops due to the increase in velocity, pulling the kayak to the right hand side (positive side force). The same phenomenon is observed on the left. Likewise the paddle hull interaction can clearly

be seen in all three moments. Although only initial, un-validated self propulsion data is presented, the potential benefits of this type of analysis is clear.

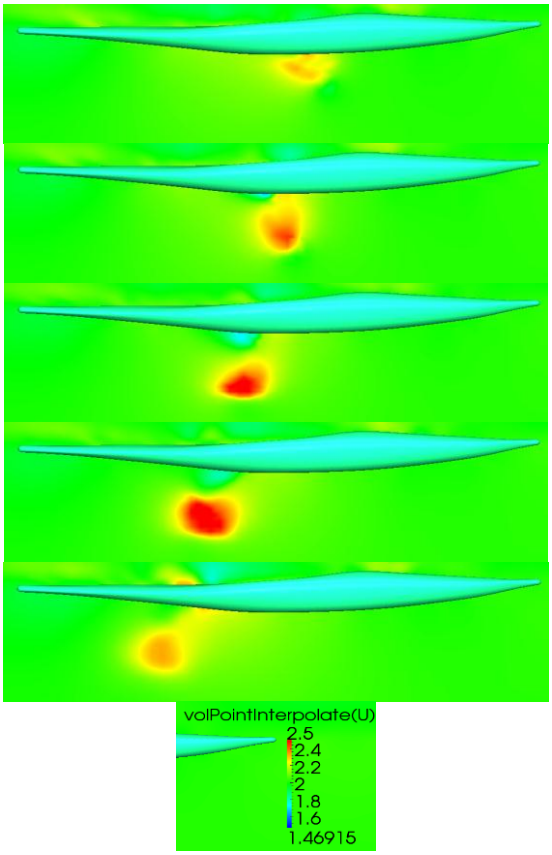

Figure 4-4 - Paddle induced velocities throughout a single paddle stroke, viewed on a plane placed through the centre of rotation of the paddle.

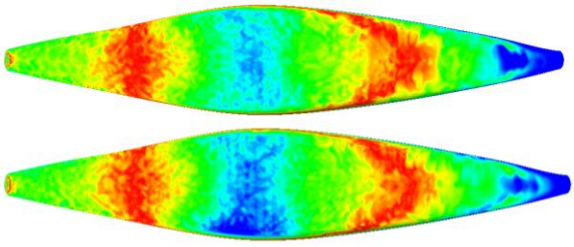

Figure 4-5 - hydrodynamic pressure field on the bottom of the kayak (naked hull above, as paddle blade passes below).

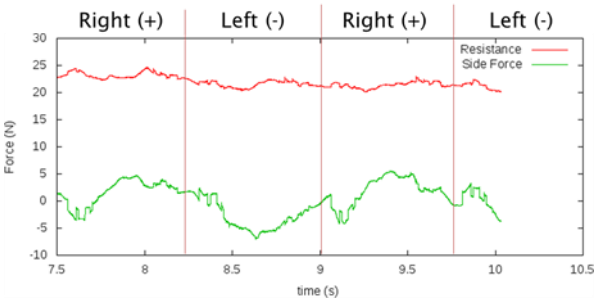

Figure 4-6 - Self propelled hydrodynamic forces acting on the kayak

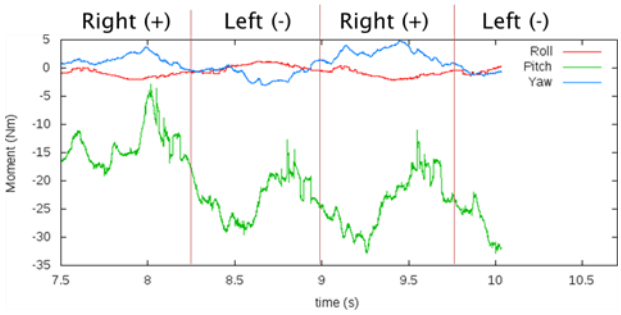

Figure 4-7 - Moments induced by the self propelled forces.

5 Conclusions

A simplified mathematical model of a paddle has been used to simulate a paddle stroke using a body force method. Experimental data has been used to validate the model and refine the drag coefficients used until improvements to the mathematical model can be included.

An initial self propelled kayak simulation has been performed using the developed methodology, which highlights the significant impact the paddle stroke has on the kayak's fluid dynamic forces.

6 References

Ellison, W., Turnock, S.R., (2010) Investigation into the effect of the kayak paddle stroke on elite kayak performance, Ship Science Individual Project, School of Engineering Sciences, University of Southampton, UK.

Hino T. (2005) CFD Workshop Tokyo 2005. In: The Proceedings of CFD Workshop Tokyo.

Hoerner, S.F., (1965) Fluid-Dynamic Drag. 3-16. Published by the author, Midland Park, NJ

Larsson L, Stern F, Bertram V. (2003) Benchmarking of Computational Fluid Dynamics for Ship Flows: The Gothenburg 2000 Workshop. Journal of Ship Research 2003;47:63–81(19).

Menter, F.R., (1994) Two-equation eddy-viscosity turbulence models for engineering applications. AIAA Journal 32(8):1598 –605.

OpenFOAM®, (2009) OpenFOAM – The Open Source CFD Toolbox- User Gide, Version 1.6.

Peric, M., Ferziger, J.H., (2002) Computational Methods for Fluid Dynamics, Springer, 3rd edition.

Phillips, A.B., Turnock, S.R. and Furlong, M.E. (2010) Accurate capture of rudder-propeller interaction using a coupled blade element momentum-RANS approach. *Ship Technology Research (Schiffstechnik)*, 57, (2), 128-139.